

**Technical Report
1069**

Aperture Sampling Limitations of Linear and Circular Arrays for Direction Finding and Nulling

D.A. Shnidman

14 May 2002

Lincoln Laboratory
MASSACHUSETTS INSTITUTE OF TECHNOLOGY
LEXINGTON, MASSACHUSETTS



Prepared for the Department of Defense under Air Force Contract
F19628-00-C-0002.

Approved for public release; distribution is unlimited.

20020603 078


This report is based on studies performed at Lincoln Laboratory, a center for research operated by Massachusetts Institute of Technology. The work was sponsored by the Department of Defense under Air Force Contract F19628-00-C-0002.

This report may be reproduced to satisfy needs of U.S. Government agencies.

The ESC Public Affairs Office has reviewed this report, and it is releasable to the National Technical Information Service, where it will be available to the general public, including foreign nationals.

This technical report has been reviewed and is approved for publication.

FOR THE COMMANDER


Gary Tutungian
Administrative Contracting Officer
Plans and Programs Directorate
Contracted Support Management

Non-Lincoln Recipients

PLEASE DO NOT RETURN

Permission is given to destroy this document
when it is no longer needed.

Massachusetts Institute of Technology
Lincoln Laboratory

**Aperture Sampling Limitations of Linear and Circular
Arrays for Direction Finding and Nulling**

*D.A. Shnidman
formerly Group 44*

Technical Report 1069

14 May 2002

Approved for public release; distribution is unlimited.

ABSTRACT

Is there an upper limit to the number of elements or, equivalently, samples, that can be usefully employed for direction finding or nulling a set of incoming wavefronts within a fixed size aperture? Mathematical theory states that this number is unlimited, but this result requires a perfect knowledge of the wavefront correlation matrix (i.e., a noise- and error-free environment) and infinite precision. To answer the question realistically, one must consider the element-to-element correlation matrix resulting from a set of incoming wavefronts impinging on an array of antenna elements. This matrix becomes ill-conditioned as the number of elements within the aperture increases.

This report shows that each eigenvalue associated with the correlation matrix equals the sum of the powers of all the wavefronts projected onto the dimension represented by its corresponding eigenvector. If the eigenvalue is of negligible power and easily lost in noise and other causes of data corruption, then the essential information associated with that eigenvector, and the dimension it represents, is lost. Elements corresponding to the number of small eigenvalues are of little value for the given set of wavefronts. The results must be generalized by choosing a set of wavefronts that encompasses the entire range of interest so that if an element is of questionable value for this "testing wavefront," then it has doubtful value for any set of wavefronts. Using the testing wavefront, an upper bound can be determined to the number of useful elements that can be employed within a specified fixed aperture.

TABLE OF CONTENTS

Abstract	iii
List of Illustrations	vii
1. INTRODUCTION	1
2. BACKGROUND	3
3. DETERMINING SAMPLING LIMITS	7
4. UNIFORM ARRAYS	11
5. NONUNIFORM ARRAYS	15
5.1 Log-Periodic Spacing	15
5.2 Random Spacing	15
6. CIRCULAR ARRAYS	21
7. FUTURE WORK	27
8. CONCLUSIONS	29
REFERENCES	31
APPENDIX – EMITTER AND JAMMER DATA SETS	33

LIST OF ILLUSTRATIONS

Figure No.		Page
1	Eigenvalue rolloff versus m for $M = 6-10$, $A/\lambda = 1$, uniform array, testing wavefront.	11
2	Eigenvalue rolloff versus m for $M = 7-11$, $A/\lambda = 2$, uniform array, testing wavefront.	12
3	Eigenvalue rolloff versus m for $M = 9-13$, $A/\lambda = 3$, uniform array, testing wavefront.	12
4	Eigenvalue rolloff versus m for $M = 11$, $A/\lambda = 2$, $W = 45^\circ, 60^\circ, 75^\circ$, and 90° , uniform array, testing wavefront.	13
5	Eigenvalue rolloff versus m for $M = 6-10$, $A/\lambda = 1$, log-periodic array, testing wavefront.	16
6	Eigenvalue rolloff versus m for $M = 7-11$, $A/\lambda = 2$, log-periodic array, testing wavefront.	16
7	Eigenvalue rolloff versus m for $M = 9-13$, $A/\lambda = 3$, log-periodic array, testing wavefront.	17
8	Eigenvalue rolloff versus m for $M = 11$, $A/\lambda = 2$, $W = 45^\circ, 60^\circ, 75^\circ$, and 90° , log-periodic array, testing wavefront.	17
9	Eigenvalue rolloff versus m for $M = 6-10$, $A/\lambda = 1$, random array, testing wavefront.	18
10	Eigenvalue rolloff versus m for $M = 7-11$, $A/\lambda = 2$, random array, testing wavefront.	18
11	Eigenvalue rolloff versus m for $M = 9-13$, $A/\lambda = 3$, random array, testing wavefront.	19
12	Eigenvalue rolloff versus m for $M = 11$, $A/\lambda = 2$, $W = 45^\circ, 60^\circ, 75^\circ$, and 90° , random array, testing wavefront.	19
13	Eigenvalue rolloff for the circular array, $r = 0.3\lambda$, testing wavefront, $M = 5, 6, 7$, and 8 .	23
14	Eigenvalue rolloff for the circular-0 array, $r = 0.3\lambda$, testing wavefront, $M = 5, 6, 7$, and 8 .	24
15	Eigenvalue rolloff for the circular array, $r = 0.3\lambda$, testing wavefront, and three jammer scenarios, $M = 6$.	24
16	Eigenvalue rolloff for the circular-0 array, $r = 0.3\lambda$, testing wavefront, and three jammer scenarios, $M = 6$.	25

1. INTRODUCTION

How many antenna array elements (samples) are beneficial for direction finding or nulling with a fixed aperture size? Mathematically, additional elements are beneficial; however, perfect knowledge of the ideal correlation matrix and infinite precision are required. With finite precision, finite time averaging, finite signal to noise, finite dynamic range, radio frequency interference, antenna element coupling, nonuniform directional background noise, and pattern distortions, the number of useful elements is compromised. To answer the question realistically, the correlation matrix resulting from a set of incoming wavefronts is considered; the matrix becomes ill-conditioned as the number of elements increases within the aperture. Each eigenvalue associated with the correlation matrix corresponds to the power sum of all the wavefronts projected onto the dimension represented by its corresponding eigenvector. If the eigenvalue is of negligible power and easily lost in noise and other causes of data corruption, then the essential information associated with that dimension is lost. By reducing the number of elements to correspond to the number of significant eigenvalues and suitably positioning the remaining elements within the specified aperture, little information regarding the set of wavefronts is lost.

The result is generalized by postulating a set of wavefronts that encompasses the entire range of interest; if an element has questionable values for this wavefront set, designated the testing wavefront, then it has doubtful value for any set of wavefronts. Using the testing wavefront, an upper bound can be determined to the number of useful elements that can be employed within a specified fixed aperture.

Linear arrays of fixed aperture are considered, then generalized to two-dimensional circular arrays. This report is confined to linear and circular arrays, but the technique can be applied to more general (e.g., three-dimensional) arrays.

2. BACKGROUND

Considered here is a linear array of M isotropic antenna elements positioned at locations d_m along the x -axis. The M vector of baseband receiver outputs at a sampling time, t_i , due to the k th narrowband received signal of wavelength λ and planewave direction θ_k off broadside to the axis, is

$$\underline{X}_k(t_i) = s_k(t_i) \underline{V}'(z'_k) \quad ,$$

where the complex scalar $s_k(t_i)$ represents the amplitude and phase of the received signal at element one (using reference element $m = 1$ so that $d_1 = 0$). $\underline{V}'(z'_k)$ is the M -dimensional vector of samples that is referred to as the “response vector” and defined by

$$\underline{V}'(z'_k) = (1, z'_k(d_2), z'_k(d_3), \dots, z'_k(d_M))^T \quad ,$$

where, in turn,

$$z'_k(d_m) = \exp(-j2\pi d_m \sin \theta_k / \lambda)$$

so that $z'_k(d_1) = 1$. The $s_k(t_i)$ are modeled as zero-mean, independent (in both k and i) random sequences of stationary statistics.

Uniform linear arrays are considered first, then generalized to nonuniform and two-dimensional arrays. For the uniform array, $d_m = (m-1)d$, where d is the common separation between elements. In this case, $z'_k(d_2)$ becomes z_k and $z'_k(d_m) = z_k^{m-1}$, where

$$z_k = \exp(-j2\pi d / \lambda \sin \theta_k) \quad .$$

The response vector, $\underline{V}'(z_k)$, then simplifies to $\underline{V}(z_k)$, where

$$\underline{V}(z_k) = (1, z_k, z_k^2, \dots, z_k^{(M-1)})^T \quad .$$

This latter vector $\underline{V}(z_k)$ is called a Vandermonde vector. In this case \underline{V}_k represents $\underline{V}(z_k)$. Any distinct set of M or fewer Vandermonde M -dimensional vectors is linearly independent. In order that no two off-broadside angles, θ_k , share the same value of z_k , d must be no larger than $\lambda/2$.

If there were K signal wavefronts ($K < M$) impinging on the array, the vector of receiver outputs at time t_i would be

$$\underline{X}(t_i) = \underline{n}(t_i) + \sum_{k=1}^K \underline{X}_k(t_i) \quad , \quad (1)$$

where $\underline{n}(t_i)$ is the M vector of internal receiver noise and other noise sources, which for this analysis are assumed independent from receiver to receiver and of average power level σ^2 in each receiver.

The correlation (covariance) matrix, R , is obtained by averaging the $M \times M$ outer product $\underline{X}_k(t_i)\underline{X}_k(t_i)^H$, where the H operator is the conjugate transpose. It is assumed that the signal wavefronts are all uncorrelated so that

$$E\{\underline{X}_k(t_i)\underline{X}_j^H(t_i)\} = 0 \quad \text{for } k \neq j \quad . \quad (2)$$

With this signal model, the expectation for the R matrix becomes

$$R = E\{\underline{X}(t_i)\underline{X}(t_i)^H\} = VPV^H + \sigma^2 I \quad ,$$

where P is a $K \times K$ diagonal matrix with diagonal terms ρ_k , which, in turn, are given by

$$\rho_k = E\{|S_k(t_i)|^2\}, \quad \text{for } k = 1, 2, \dots, K \quad . \quad (3)$$

V is an $M \times K$ matrix having columns that are K Vandermonde vectors, each column corresponding to a signal direction. The signal-dependent component of the R matrix, S , can be spectrally decomposed to

$$S = VPV^H = \sum_{k=1}^K \rho_k \underline{V}_k \underline{V}_k^H \quad (4)$$

to obtain

$$S = VPV^H = \sum_{k=1}^K \lambda_k \underline{u}_k \underline{u}_k^H \quad . \quad (5)$$

Note that the subscripted λ s refer to eigenvalues, whereas the unsubscripted λ refers to wavelength. The K Vandermonde vectors span a space, S_K , of dimension K . The M eigenvectors, \underline{u}_m , span a space S_M of dimension M . The space spanned by S_K for $K < M$ is a subspace of S_M . The space S_K is referred to as the

“signal subspace” that is identical to the space spanned by the K eigenvectors of S having nonzero eigenvalues. The remaining $M-K$ dimensional subspace is the noise space. Since all the eigenvectors of a Hermitian matrix are mutually orthogonal, the Vandermonde vectors are each orthogonal to the noise subspace. The noise space can be used to direction find up to $M-1$ wavefronts.

In an ideal situation, S is obtained from R by subtracting $\sigma^2 I$. In reality, there is no R , but it can be estimated with a sampled version, R' , by averaging $\underline{X}_k(t_i)\underline{X}_k(t_i)^H$ over, say L samples,

$$R' = \frac{1}{L} \sum_{i=1}^L \underline{X}(t_i) \underline{X}^H(t_i) = V P E^H + E, \quad (6)$$

where, for the error matrix, E , is

$$E = \begin{bmatrix} \sigma_1^2 & \epsilon_{12} & \cdots & \epsilon_{1M} \\ \epsilon_{21} & \sigma_2^2 & \cdots & \epsilon_{2M} \\ & & \cdots & \\ \epsilon_{M1} & \epsilon_{M2} & \cdots & \sigma_M^2 \end{bmatrix} \quad (7)$$

and where L is as large as practical.

For the ideal case, E is simplified to $\sigma^2 I$. If it is assumed that the K wavefronts are incoherent, then the signal cross-terms in R' average down to near zero, leaving, essentially, the signal self-terms. The independence of the noise terms causes both the noise cross-terms and the signal-noise cross-terms to average down to nearly zero so that the ϵ_{mn} terms should all be close to zero.

If all the element patterns and receivers are identical, then the σ_m^2 are about equal, giving $R \approx R'$. To ascertain the estimate of S , a value must be determined to be used for σ^2 , and $\sigma^2 I$ must be subtracted from R' . In the ideal case this step is relatively easy because with $K < M$, the noise eigenvalues of R are all σ^2 . Instead, there is R' , and since E has nonzero off-diagonal terms and the σ_m^2 are not identical on the diagonal, the choices for K and σ^2 are usually not obvious [1–5]. With one nonzero pair, $\epsilon_{mn} = \epsilon_{nm}^* \neq 0$, each eigenvalue is shifted by an amount proportional to ϵ_{mn} with the proportionality factors summing to one [6]. Critical information in the eigenvalues and eigenvectors is thereby corrupted. A typical noise/distortion floor is expected to be in the range of 30 dB below the peak signal-to-noise ratio (SNR). With precision calibration, a further reduction can be expected on the order of 15 to 20 dB, which is the current limit, but even if a 10 dB improvement is allowed, it would make a difference of no more than one useful sample. As a result, most systems will have difficulty distinguishing between signal and noise eigenvalues due to distortions and nonuniform noise when the λ_m are about 40 dB below the largest signal

eigenvalue. For the most optimistic situation, another 10 to 15 dB may be allowed, which might admit one or two more useful samples; the number of useful elements, or samples, is, therefore, limited.

3. DETERMINING SAMPLING LIMITS

Information about the signal waveforms impinging on the array is obtained from the larger eigenvalues and the corresponding eigenvectors of the S matrix. A correlation matrix must be constructed that ultimately will allow the determination of the number of useful samples; i.e., the useful number of elements in the array for a given aperture size in wavelengths. A Vandermonde vector, \underline{V}_k , is expanded in terms of the eigenvectors of S , to obtain

$$\underline{V}_k = \sum_{m=1}^M \alpha_{km} \underline{u}_m, \quad \text{where } \alpha_{km} = \underline{u}_m^H \underline{V}_k \quad (8)$$

so that the α_{km} are the projections of the k th Vandermonde on the m th eigenvector. By definition,

$$\lambda_m = \underline{u}_m^H S \underline{u}_m$$

so that

$$\begin{aligned} \lambda_m &= \underline{u}_m^H S \underline{u}_m = \underline{u}_m^H \left[\sum_{k=1}^K \rho_k \underline{V}_k \underline{V}_k^H \right] \underline{u}_m \\ &= \sum_{k=1}^K \rho_k (\underline{u}_m^H \underline{V}_k) (\underline{V}_k^H \underline{u}_m) = \sum_{k=1}^K \rho_k |\alpha_{km}|^2. \end{aligned} \quad (9)$$

Each eigenvalue is equal to the sum of the projected powers of all the Vandermondes onto its eigenvector [see Equation (9)]. Small eigenvalues correspond to dimensions in which there is almost no power from any wavefront. In an ideal case, any nonzero level is satisfactory for extracting information, which is not true in the real environment, where S is not known. Note that if eigenvalues are too small, they cannot be determined with good accuracy, and the coordinates corresponding to their eigenvectors provide no useful information [see Equation (9)]. Therefore, fewer coordinate axes, i.e., fewer samples, would be as useful, less complicated, and less expensive.

If interest is in a specific set of wavefronts, the corresponding correlation matrix can be formed and its eigenvalue rolloff analyzed. Generally, however, a set of wavefronts must be selected that generate a matrix S that allows one to determine, for a given aperture, coverage region, and signal spatial distribution, the maximum number of useful samples that can be taken under some total noise/distortion

level assumption. The resulting eigenvalue rolloff then gives an upper bound to the number of useful elements/samples for a particular signal spatial distribution.

Given that it is not desirable to artificially limit the number of significant eigenvalues due to lack of signals, a set of wavefronts must be selected with $K > M$ and, preferably, $K \gg M$, as well as choosing signal wavefronts that will not bias the results. To achieve this end, the signal directions and the signal power levels are made uniform ($P = I$) so that identical signal plane waves uniformly cover the entire region. The resulting set of wavefronts is referred to as the “testing wavefront.” The intent is to manufacture a covariance having as many high eigenvalues as possible. With M as the number of antenna elements, A/λ as the aperture in wavelengths, and $-W$ to W ($W \leq \pi/2$) as the coverage region, S is

$$S = \sum_{k=1}^K \rho_k \underline{V}_k \underline{V}_k^H \triangleq [s_{mn}] \quad , \quad (10)$$

with

$$s_{mn} = \frac{1}{2W} \sum_{k=-W/\delta\phi}^{W/\delta\phi} e^{-j2\pi \frac{(m-n)A}{(M-1)\lambda} \sin(k\delta\phi)} \delta\phi \quad , \quad (11)$$

where signals are separated by an angle $\delta\phi$. If $\delta\phi$ approaches zero, then, since $K\delta\phi = W$, s_{mn} approaches

$$s_{mn} = \frac{1}{2W} \int_{-W}^W e^{-j2\pi \frac{(m-n)A}{(M-1)\lambda} \sin\phi} d\phi \quad . \quad (12)$$

The Bessel function identity [7, #9.1.41 with $t = \exp(-j\alpha)$]

$$e^{-jz \sin\alpha} = \sum_{p=-\infty}^{\infty} e^{-j p \alpha} J_p(z) \quad (13)$$

can be used in Equation (12) to obtain, after changing the order of integration and summation,

$$\begin{aligned}
s_{mn} &= \frac{1}{2W} \sum_{p=-\infty}^{\infty} J_p \left(\frac{2\pi A(m-n)}{\lambda(M-1)} \right) \int_{-W}^W e^{-j p \phi} d\phi \\
&= \sum_{p=-\infty}^{\infty} J_p \left(\frac{2\pi A(m-n)}{\lambda(M-1)} \right) \frac{\sin(pW)}{pW} .
\end{aligned} \tag{14}$$

With the identity [7, #9.1.5]

$$J_{-p}(z) = (-1)^p J_p(z) . \tag{15}$$

Equation (14) can be written

$$s_{mn} = J_0 \left(2\pi \frac{A(m-n)}{\lambda(M-1)} \right) + 2 \sum_{\substack{p=2 \\ p \text{ even}}}^{\infty} J_p \left(2\pi \frac{A(m-n)}{\lambda(M-1)} \right) \frac{\sin(pW)}{pW} \tag{16}$$

and note that for $W = \pi/2$ (90°), s_{nm} simplifies to the J_0 term only. For a nonuniform array, with the m th element located at d_m and $A = d_M - d_1$, the result in Equation (16) is generalized to

$$s_{mn} = J_0 \left(\frac{2\pi}{\lambda} (d_m - d_n) \right) + 2 \sum_{\substack{p=2 \\ p \text{ even}}}^{\infty} J_p \left(\frac{2\pi}{\lambda} (d_m - d_n) \right) \frac{\sin(pW)}{pW} . \tag{17}$$

Since the testing wavefront contains fronts from more directions than most practical scenarios, eigenvalues are expected to have more sources contributing to their value, they roll off more slowly, and an upper bound to the count is being produced.

For a uniform array, $s_{mn} = s_{mn}(M, A/\lambda, W)$ is a function of three parameters; M is the number of samples (or, equivalently, elements); A/λ is the aperture (in wavelengths), and the observation range is $-W$ to W . The investigation of signal space behavior and its eigenvalues begins for the cases in which the array is uniform and $W = \pi/2$ (90°) and generalizes the results to other cases. The intent is that the resulting S matrices should have the slowest eigenvalue drop-off for the given parameters, hence the most measurable eigenvalues. Any other signal arrangement produces a set of eigenvalues that roll off more quickly.

4. UNIFORM ARRAYS

Generated first are the S matrices for $W = \pi/2(90^\circ)$, a set of A/λ s, and a sequence of different values of M . Eigenvalues are arranged in decreasing order for each case, and the rolloffs of these eigenvalues are examined. Figure 1 shows $A/\lambda = 1$ and M varying from 6 to 10. Note that, as far as they can, the relative eigenvalues follow almost identical rolloff sequences, nearly independent of M . Figures 2 and 3 show similar results for $A/\lambda = 2$ and $A/\lambda = 3$.

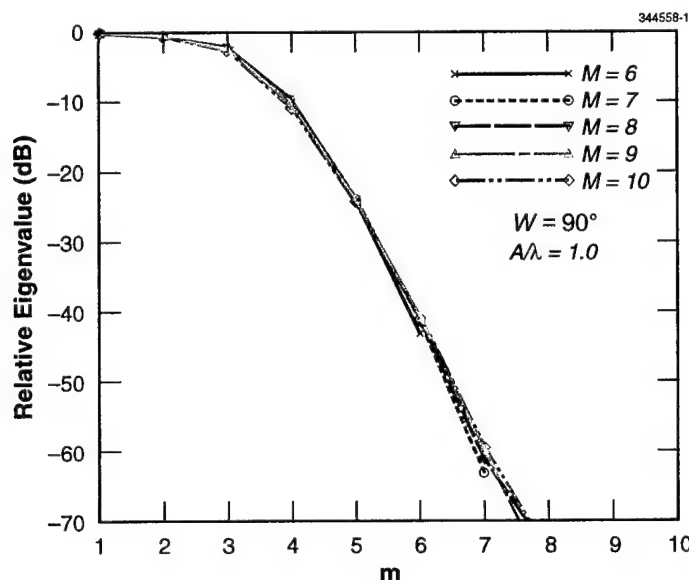


Figure 1. Eigenvalue rolloff versus m for $M = 6-10$, $A/\lambda = 1$, uniform array, testing wavefront.

An important property in all cases is that as M increases and the spacing between elements falls well below $\lambda/2$, the S matrix becomes increasingly ill conditioned; with increasing M , some eigenvalues become too small to allow an accurate calculation of the required projection coefficients. The dimension number beyond which the rolloff becomes rapid is dependent on the aperture of the array and W ; the larger the aperture, the larger the dimension number at the knee in the curve. Since the knee is ever present, a definite limit exists to the number of useful elements that can be packed into a fixed-size aperture.

Holding $A/\lambda = 2$ and $M = 11$, W is reduced to $5\pi/12$ (75°), $\pi/3$ (60°), and $\pi/4$ (45°) and results are determined with the change in W . Figure 4 shows that the drop-off occurs somewhat earlier as W decreases, but the results are not particularly sensitive to changes in W . The slowest rolloff occurs when $W = \pi/2$ (90°), i.e., the maximum number of useful samples for a given threshold level.

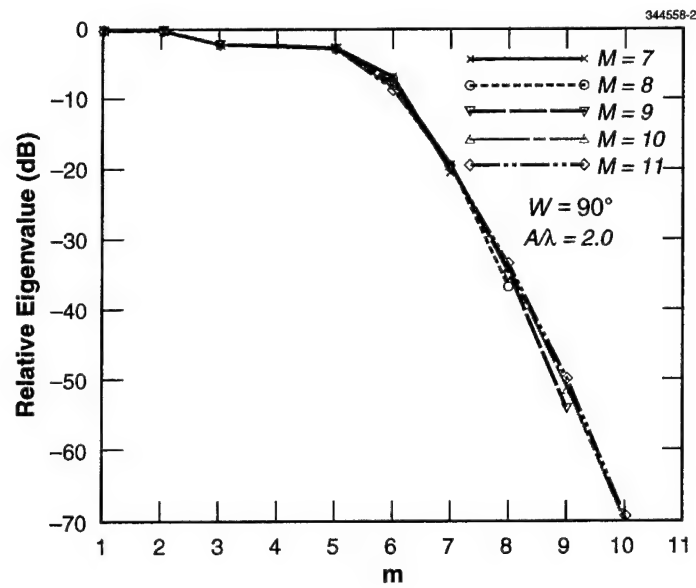


Figure 2. Eigenvalue rolloff versus m for $M = 7-11$, $A/\lambda = 2$, uniform array, testing wavefront.

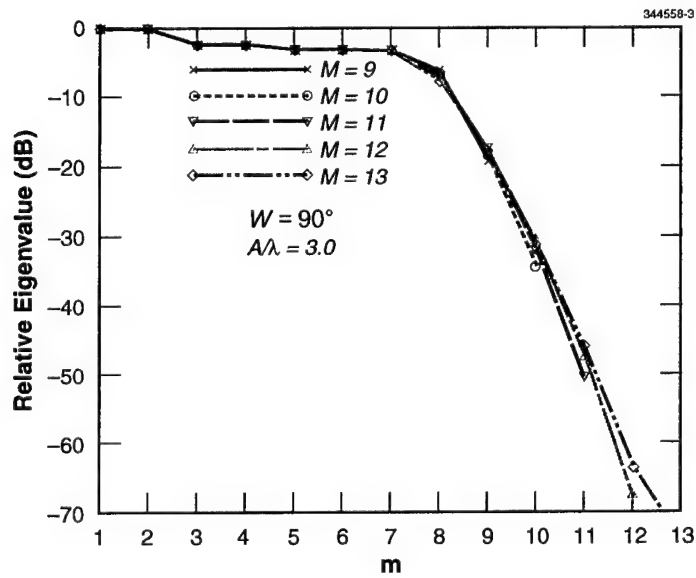


Figure 3. Eigenvalue rolloff versus m for $M = 9-13$, $A/\lambda = 3$, uniform array, testing wavefront.

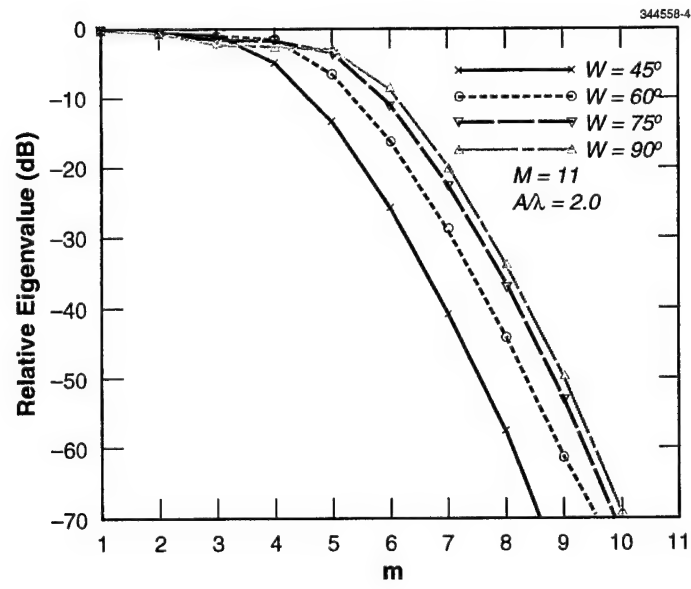


Figure 4. Eigenvalue rolloff versus m for $M = 11$, $A/\lambda = 2$, $W = 45^\circ$, 60° , 75° , and 90° , uniform array, testing wavefront.

5. NONUNIFORM ARRAYS

Each element location, d_m , must be specified for the nonuniform array. S matrices are generated using Equation (17) in place of (15). While the S matrices were symmetric and Toeplitz for uniform arrays, these general S matrices are not Toeplitz.

It was shown earlier that the $W = \pi/2$ (90°) cases produce the slowest rolloff and that the results are not sensitive to the choice of W . Initially, different cases with $W = \pi/2$ (90°) are considered for the nonuniform array. To guarantee that these arrays cover the full aperture, element one is at position zero and element M at position A . Even though most nonuniform arrays are designed to thinly or sparsely sample an aperture, it is being oversampled here to show that the sampling results obtained for uniformly spaced arrays are not dependent on uniform sampling. Two well-known nonuniform spacings are considered—log-periodic and random.

5.1 LOG-PERIODIC SPACING

Log-periodic (more precisely, periodic log-frequency) spacing specifies most element locations as scaled by a constant factor, “ a ” ($a > 1$), from the previous location. The first element, d_1 , is at zero. The next, d_2 , is arbitrary. The third and all subsequent elements are scaled by “ a ” so that $d_3 = ad_2$, $d_4 = ad_3 = a^2d_2$, etc, with $d_M = a^{M-2}d_2$ being at the aperture point A . The separation, $d_3 - d_2 = (a - 1)d_2$ is less than d_2 if $a < 2$ and would then be the smallest spacing, preferably $\leq \lambda/2$.

The results for this array are given in Figures 5–7. The same behavior as the uniform array is seen except that the rapid fall-off is somewhat greater than with the uniform array, indicating that, for a dense array with average spacing less than $\lambda/2$, the uniform array is the better arrangement. Figure 8 is an example of the eigenvalue fall-off for different W s. Results are very similar to the uniform case. Note that log-period spacing is usually adopted for sparse arrays where economy in the number of elements is a primary issue.

5.2 RANDOM SPACING

Except for the extreme, elements are randomly placed within the aperture; therefore, if there are nine elements, two are fixed-end positions, with seven randomly placed between them for a uniform distribution. Results are shown in Figures 9–11 and are almost identical to those of the log-periodic spacing as is the varying W example given in Figure 12. Both nonuniform arrays exhibit behavior similar to the uniform array. There is clearly a practical limit to the number of useful samples for linear arrays.

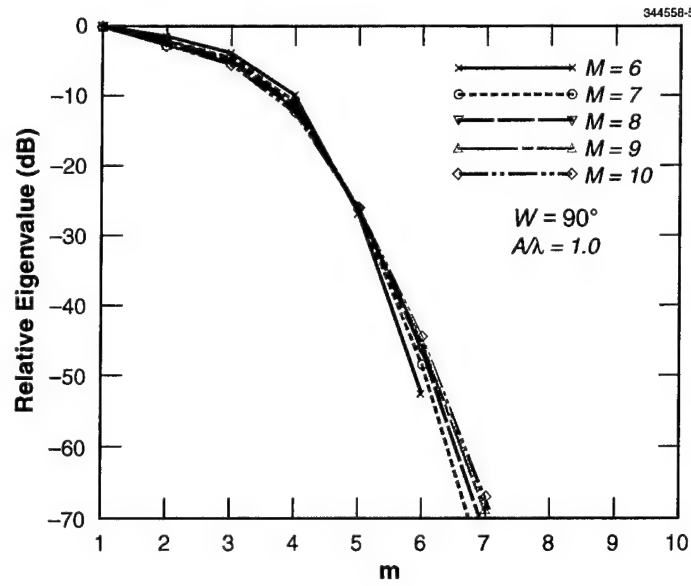


Figure 5. Eigenvalue rolloff versus m for $M = 6-10$, $A/\lambda = 1$, log-periodic array, testing wavefront.

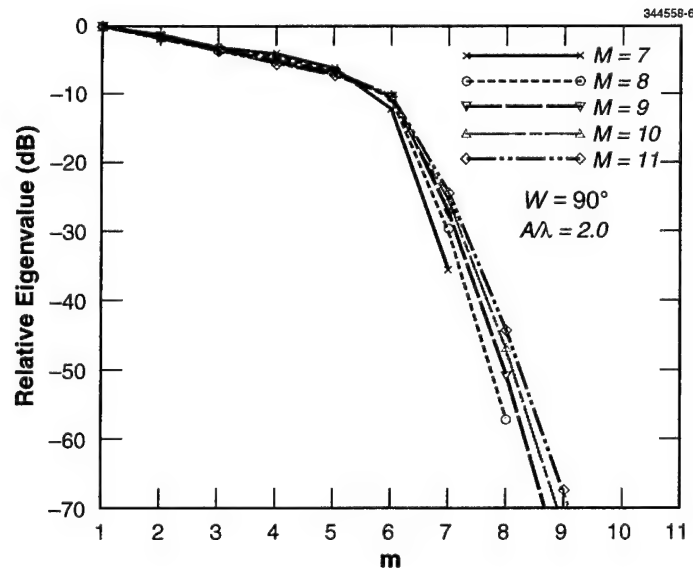


Figure 6. Eigenvalue rolloff versus m for $M = 7-11$, $A/\lambda = 2$, log-periodic array, testing wavefront.

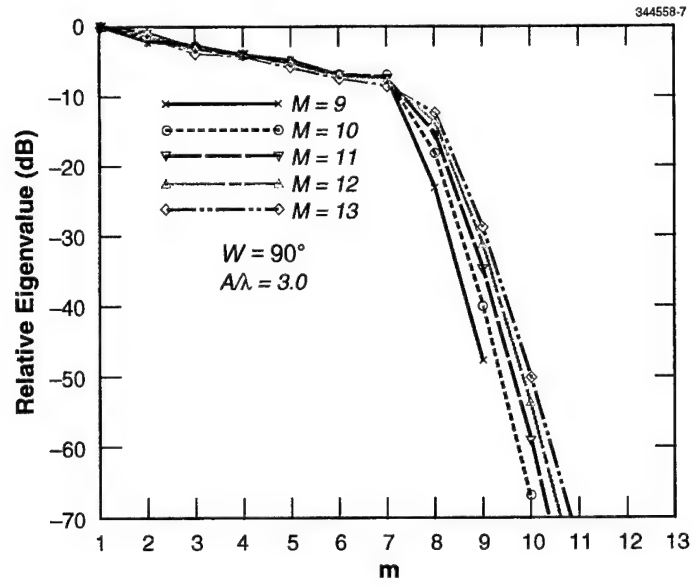


Figure 7. Eigenvalue rolloff versus m for $M = 9-13$, $A/\lambda = 3$, log-periodic array, testing wavefront.

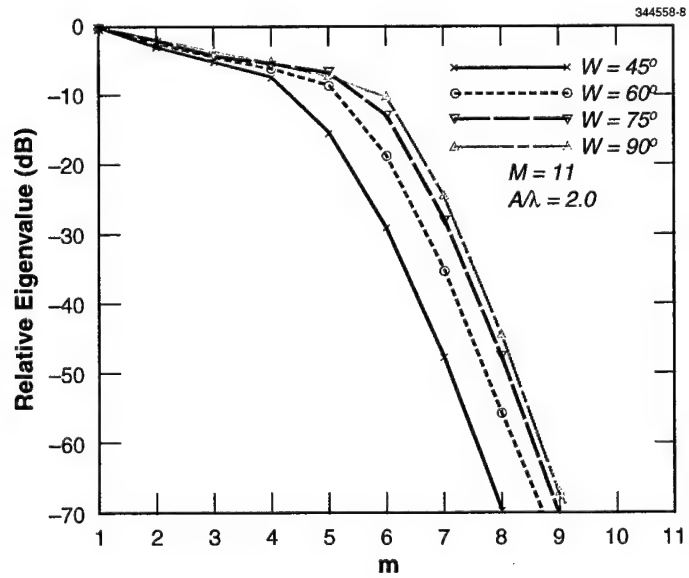


Figure 8. Eigenvalue rolloff versus m for $M = 11$, $A/\lambda = 2$, $W = 45^\circ, 60^\circ, 75^\circ$, and 90° , log-periodic array, testing wavefront.

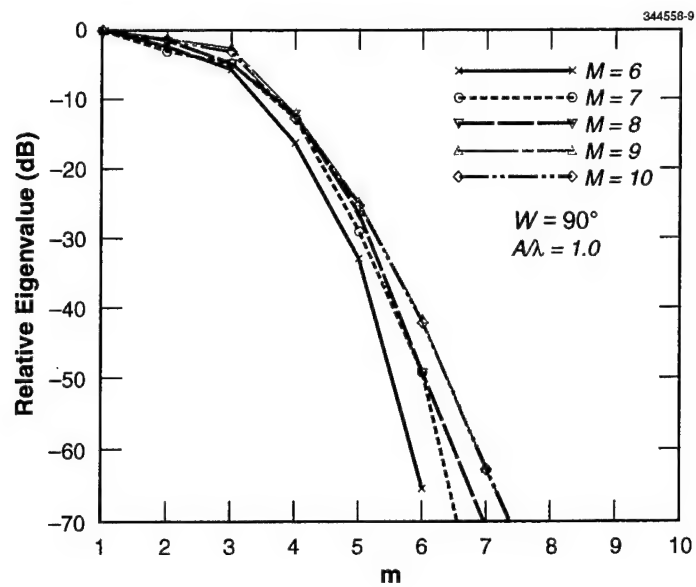


Figure 9. Eigenvalue rolloff versus m for $M = 6-10$, $A/\lambda = 1$, random array, testing wavefront.

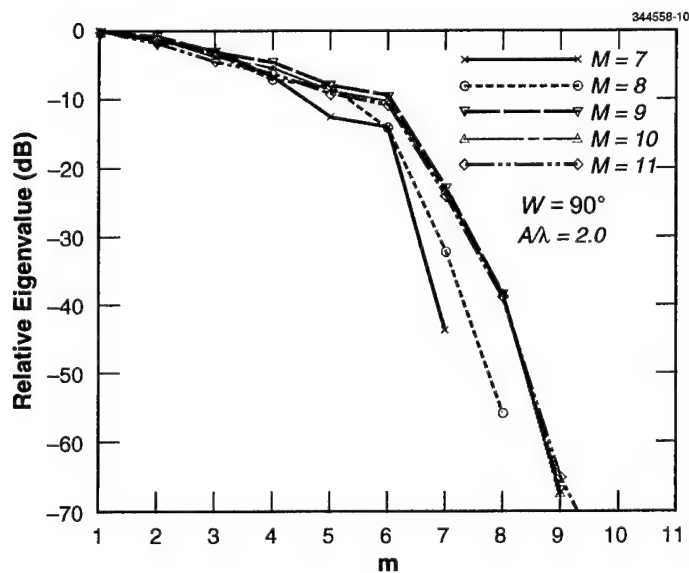


Figure 10. Eigenvalue rolloff versus m for $M = 7-11$, $A/\lambda = 2$, random array, testing wavefront.

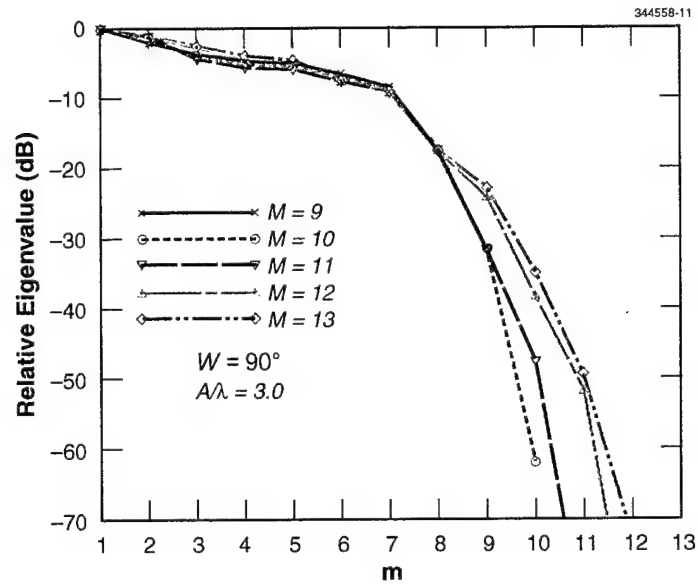


Figure 11. Eigenvalue rolloff versus m for $M = 9-13$, $A/\lambda = 3$, random array, testing wavefront.

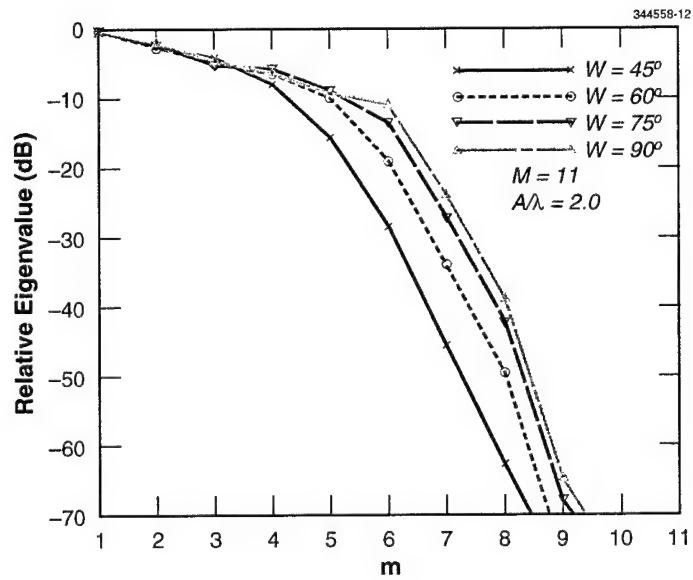


Figure 12. Eigenvalue rolloff versus m for $M = 11$, $A/\lambda = 2$, $W = 45^\circ$, 60° , 75° , and 90° , random array, testing wavefront.

6. CIRCULAR ARRAYS

Arrays with two- or three-dimensional apertures can also be investigated. For a general three-dimensional array with elements at position \underline{d}_m , where

$$\underline{d}_m^T = (x_m, y_m, z_m) \quad ,$$

and \underline{n} is the direction vector (ϕ is the spherical azimuth angle and θ the spherical elevation angle)

$$\underline{n}^T = (\cos \phi \sin \theta, \sin \phi \sin \theta, \cos \theta) \quad , \quad (18)$$

the response vectors become

$$\underline{V}'(z_k) = (1, z'_k(\underline{d}_2), z'_k(\underline{d}_3), \dots, z'_k(\underline{d}_M))^T \quad ,$$

where, in turn,

$$z'_k(\underline{d}_m) = \exp(-j2\pi(\underline{d}_m \cdot \underline{n})) \quad .$$

Then the terms of S, s_{mn} , become

$$s_{mn} = \frac{1}{2W} \frac{1}{U} \int_0^U \int_{-W}^W e^{-j2\pi/\lambda[(\underline{d}_m \cdot \underline{n}) - (\underline{d}_n \cdot \underline{n})]} d\phi d\theta \quad , \quad (19)$$

where 0 to U is the range on the elevation angle θ . $u_x(m, n)$, $u_y(m, n)$, and $u_z(m, n)$ are defined as satisfying

$$\frac{2\pi}{\lambda} [(\underline{d}_m \cdot \underline{n}) - (\underline{d}_n \cdot \underline{n})] = u_x(m, n) \cos \phi \sin \theta + u_y(m, n) \sin \phi \sin \theta + u_z(m, n) \cos \theta \quad . \quad (20)$$

In particular, a radius r circular array in the x - y plane, with M uniformly spaced elements, gives

$$\underline{d}_m^T = r (\cos(m-1)2\pi/M, \sin(m-1)2\pi/M, 0) \quad , \quad (21)$$

and the $u_x(m, n)$ and $u_y(m, n)$ become

$$u_x(m, n) = 2\pi \frac{r}{\lambda} [\cos 2\pi(m-1)/M - \cos 2\pi(n-1)/M] \quad (22)$$

and

$$u_y(m, n) = 2\pi \frac{r}{\lambda} [\sin 2\pi(m-1)/M - \sin 2\pi(n-1)/M] \quad (23)$$

with $u_z(m, n) = 0$. For the uniform circular array, the s_{mn} become

$$s_{mn} = \frac{1}{2W} \frac{1}{U} \int_0^U \int_{-W}^W e^{-j(u_x \cos \theta + u_y \sin \theta)} d\phi d\theta \quad (24)$$

For a numeric generation of the s_{mn} used for general W and U ,

$$s_{mn} = \frac{1}{2W} \frac{1}{U} \sum_{p=0}^{U/\delta\theta} \sum_{k=-W/\delta\phi}^{W/\delta\phi} e^{-j[u_x(m, n) \cos(k\delta\phi) \sin(p\delta\theta) + u_y(m, n) \sin(k\delta\phi) \sin(p\delta\theta)]} \delta\phi \delta\theta \quad (25)$$

where, specifically,

$$u_x(m, n) = \frac{2\pi r}{\lambda} (x_m - x_n) \quad \text{and} \quad u_y(m, n) = \frac{2\pi r}{\lambda} (y_m - y_n) \quad (26)$$

Using Equation (25) for a numerical evaluation, the S matrix can be filled and the behavior of its eigenvalues examined.

The focus now turns to two circular arrays. The first has all its elements uniformly distributed on the circumference. The second (referred to as “circular-0,”) is similar to the first except that one element is placed in the center of the circle. A testing wavefront is chosen to cover a $\pm\pi/2$ ($\pm 90^\circ$) wedge in azimuth and either a $\pi/4$ (45°) or $\pi/2$ (90°) wedge in elevation. Again, the testing wavefront is expected to produce a slow eigenvalue rolloff and an upper bound to the number of useful elements. For example, the radius of the circular array is 0.3λ . A circle with a 0.3λ radius has a 1.885λ circumference. With a four-element array, the elements are separated on the circumference by approximately $\lambda/2$. As such, the eigenvalue rolloff is expected to start somewhere between five and six elements. The resulting rolloffs for four-, five-, six-, and seven-element arrays are plotted in Figure 13.

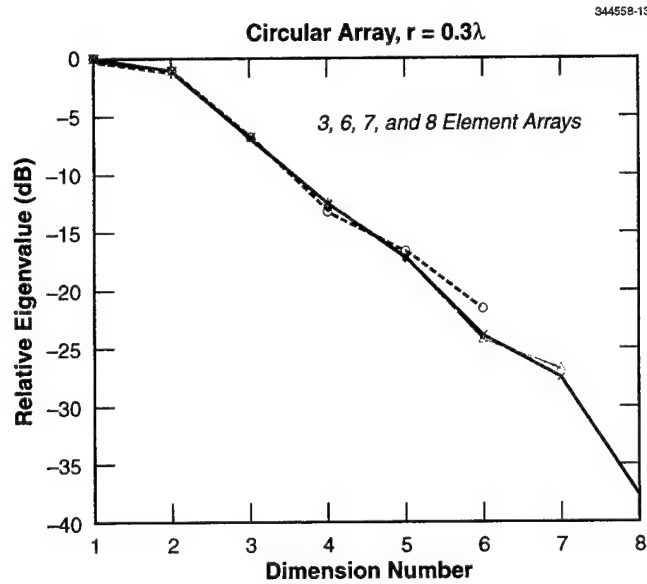


Figure 13. Eigenvalue rolloff for the circular array, $r = 0.3\lambda$, testing wavefront, $M = 5, 6, 7$, and 8 .

These results are repeated in Figure 14 for the circular-0 array. Comparing Figures 13 and 14 shows that the circular-0 arrangement is generally inferior to the circular array with the same number of elements. A heuristic argument for this result is that the center element measurement is the average of all the other element measurements and does not contain substantially new information.

From a collection of 30 scenarios that were designed to represent realistic jamming situations, three cases were examined. The resulting eigenvalue rolloffs were compared to each other and to the results of the testing wavefront. Actual jammer locations and power levels for these scenarios are given in Appendix A. For the circular array (Figure 15), the eigenvalue rolloffs for these scenarios are far more precipitous than for the testing wavefront. They indicate that only three or four samples (elements) are useful, even though each scenario has at least 27 jammers. Figure 16 shows the analogous results for the circular-0 array. The rolloff is slightly faster than for the circular array. Again, the center element appears to be of dubious value.

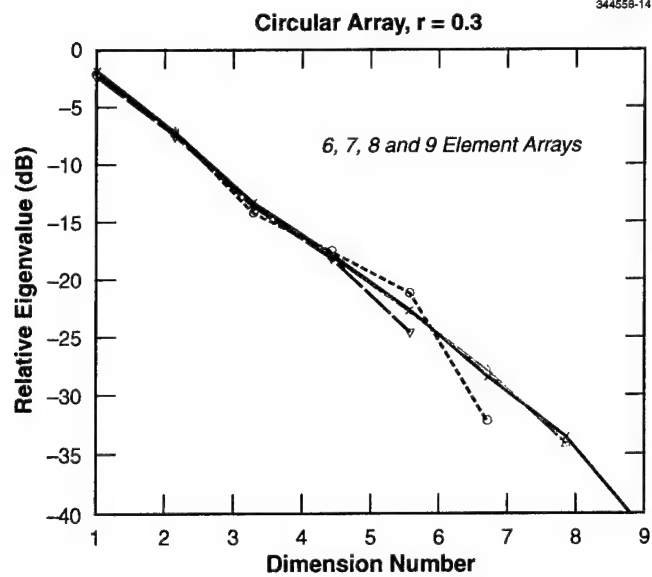


Figure 14. Eigenvalue rolloff for the circular-0 array, $r = 0.3\lambda$, testing wavefront, $M = 5, 6, 7$, and 8 .

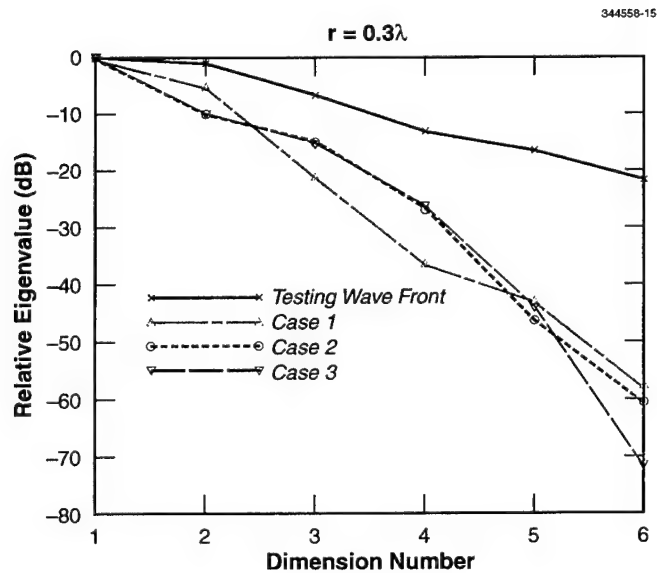


Figure 15. Eigenvalue rolloff for the circular array, $r = 0.3\lambda$, testing wavefront, and three jammer scenarios, $M = 6$.

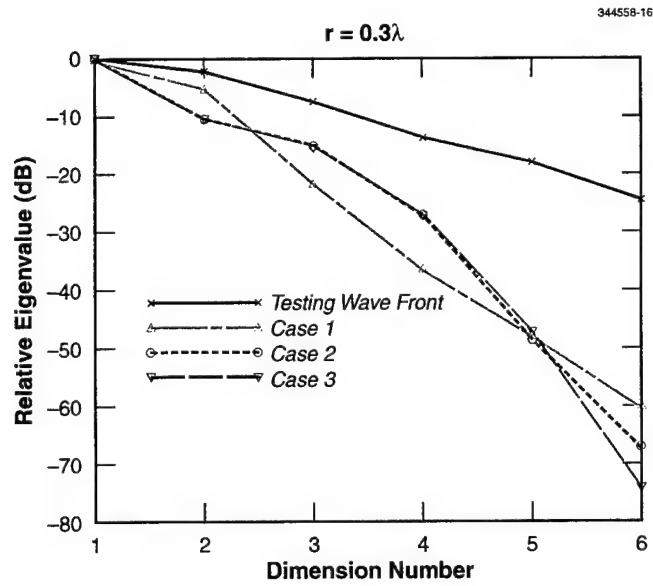


Figure 16. Eigenvalue rolloff for the circular-0 array, $r = 0.3\lambda$, testing wavefront, and three jammer scenarios, $M = 6$.

7. FUTURE WORK

When the incoming wavefronts are associated with significant multipath, STAP processing is more suitable and requires the use of tapped delay lines at each receiver to handle the correlated input [8], requiring replacement of the element correlation matrix with one that includes the output of the tapped delay lines. If there are M elements and K taps per element, then the correlation matrix would be an $M \times K$ by $M \times K$ matrix. The source or testing wavefront would need to be modified to include the characteristics of the multipath in the wavefronts; the eigenvalue rolloffs of this expanded matrix would then be the ones under investigation.

8. CONCLUSIONS

For a linear array of aperture A/λ , the number of useful elements (samples) of practical utility is limited. If the number of elements is limited to those spaced $\lambda/2$ apart, they are all useful and correspond to $2A/\lambda+1$ elements. As more and more elements are added, the correlation matrix becomes ill conditioned, implying small eigenvalues, which, in turn, imply dimensions in the signal subspace that have coefficients too small to be valuable as they will be masked by noise. This investigation was extended to circular arrays, with similar results. Clearly, there is a limit to the number of useful elements confined within a fixed aperture.

REFERENCES

1. S.M. Kay and S.L. Marple, "Spectrum Analysis—A Modern Perspective," *Proc. IEEE*, Vol. 69, 11, November 1981, 1380–1419.
2. D.W. Tufts and R. Kumaresan, "Estimation of Frequencies of Multiple Sinusoids: Making Linear Prediction Perform Like Maximum Likelihood," *Proc. IEEE*, Vol. 70, 9, September 1982, 975–989.
3. J.G. Proakis, C.M. Rader, F. Ling, and C.L. Nikias, *Advanced Digital Signal Processing*, Macmillan, N.Y., 1992, Chapter 8.
4. R.O. Schmidt, "Multiple Emitter Location and Signal Power Estimation," *IEEE Trans. Antenna Propag.*, Vol. AP 34, March. 1986, 276–280.
5. W. Xu, J. Pierre, and M. Kaveh, "Practical Detection with Calibrated Arrays," *Proc. IEEE Sixth SSAP Workshop on Statistical Signal & Array*, October 7–9, 1992, 82–85.
6. G.H. Golub and C.F. Van Loan, *Matrix Computations*, Johns Hopkins Univ. Press, Baltimore, Md., 1983, p. 270.
7. M. Abramowitz and I.A. Stegun, editors, *Handbook of Mathematical Functions with Formulas, Graphs, and Math. Tables*, National Bureau of Standards, Applied Math. Series, 55, U.S. Government Printing Office, Washington, D.C., 1964.
8. Private communication with Keith Forsythe, 15 September 2000.

APPENDIX—EMITTER AND JAMMER DATA SETS

```

% EMITTER DATA SET      case1.out
% Satellite              Az (deg)      El (deg)      Power (dBW)
if(cno == 1)
SA = [ 1,                143.49,        0.95,        -161.170;
      2,                  5.83,         9.17,        -159.800;
      3,                106.43,       64.90,        -152.330;
      4,                -15.38,       67.68,        -153.830;
      5,                110.91,       30.42,        -158.090;
      6,               -143.96,       56.83,        -154.190;
      7,                -60.71,       52.31,        -157.570];

elseif(cno==2)
% EMITTER DATA SET      case2.out
% Satellite              Az (deg)      El (deg)      Power (dBW)
SA = [ 1,                 61.56,       15.27,       -160.920;
      2,                136.12,       49.35,       -159.440;
      3,                109.83,       22.89,       -158.830;
      4,                -74.70,       66.43,       -155.860;
      5,               -148.32,       39.24,       -160.150;
      6,                 0.00,       12.38,       -158.670;
      7,                -13.04,       34.62,       -159.880;
      8,                146.16,       10.60,       -159.310];

elseif( cno == 3 )
% EMITTER DATA SET      case3.out
% Satellite              Az (deg)      El (deg)      Power (dBW)
SA = [ 1,                136.42,       69.88,       -153.800;
      2,               -177.46,       41.47,       -158.420;
      3,               -49.71,       48.92,       -156.850;
      4,               -154.15,        8.14,       -162.000;
      5,                13.72,        8.72,       -161.380;
      6,               -15.72,        0.91,       -163.230;
      7,                68.88,       51.94,       -156.580;
      8,                76.82,        7.24,       -161.480;
      9,               -124.97,       35.40,       -157.090;
      10,              -114.35,        4.76,       -161.400;];
%      11,                0.0         0.0         -130 ];

```

```
%JAMMER DATA SET      case1
if (cno == 1 )
```

%Jammer JA = [1,	Az (deg)	El (deg)	Power (dBW)
2,	56.88,	54.17,	-114.154
3,	173.15,	84.09,	-117.407
4,	42.10,	61.02,	-136.083
5,	53.14,	55.55,	-110.831
6,	37.69,	63.86,	-133.784
7,	63.75,	51.88,	-124.889
8,	49.52,	57.15,	-136.222
9,	71.28,	49.96,	-125.575
10,	41.38,	61.45,	-135.430
11,	53.35,	55.47,	-136.617
12,	36.85,	64.41,	-133.789
13,	170.71,	81.64,	-117.242
14,	174.31,	85.27,	-130.050
15,	62.51,	52.20,	-125.383
16,	53.83,	55.21,	-115.507
17,	99.88,	48.79,	-118.332
18,	-178.24,	92.31,	-122.050
19,	177.32,	88.24,	-117.136
20,	103.32,	49.15,	-119.662
21,	69.19,	50.62,	-113.307
22,	71.10,	49.62,	-105.939
23,	70.14,	50.22,	-125.200
24,	60.99,	52.23,	-106.727
25,	172.14,	82.62,	-94.359
26,	109.48,	50.29,	-118.389
27,	105.53,	49.33,	-119.938
28,	104.03,	49.25,	-119.507
29,	66.36,	51.12,	-125.195
30,	68.54,	50.57,	-125.670
31,	56.20,	54.01,	-105.094
	57.60,	53.80,	-109.896];

JAMMER DATA SET case2

elseif(cno == 2)

%Jammer	Az (deg)	El (deg)	Power (dBW)
JA = [1,	-137.93,	91.43,	-134.656
2,	173.76,	91.08,	-122.672
3,	-95.60,	92.69,	-133.532
4,	-119.64,	92.31,	-105.596
5,	-126.33,	91.74,	-134.433
6,	175.95,	90.65,	-123.497
7,	-91.89,	92.83,	-137.142
8,	-136.62,	92.44,	-119.627
9,	-130.17,	92.59,	-119.741
10,	-111.63,	92.37,	-106.919
11,	-143.27,	91.07,	-89.823
12,	-131.84,	92.15,	-121.165
13,	-107.37,	92.29,	-136.023
14,	-137.33,	92.04,	-121.078
15,	-101.21,	92.52,	-135.178
16,	-111.59,	92.37,	-132.655
17,	-132.37,	92.72,	-119.125
18,	-170.54,	90.45,	-90.893
19,	-138.08,	91.42,	-134.790
20,	171.72,	90.95,	-123.440
21,	-118.75,	91.94,	-135.436
22,	-129.76,	91.51,	-88.568
23,	174.09,	91.11,	-122.559
24,	122.17,	91.33,	-95.775
25,	-109.08,	92.29,	-134.380
26,	172.71,	91.15,	-122.376
27,	175.66,	91.10,	-122.665
28,	-116.93,	92.13,	-133.236
29,	-134.97,	92.25,	-120.430
30,	-163.70,	90.52,	-105.219
31,	-121.34,	91.88,	-134.551
32,	126.37,	91.48,	-124.411
33,	-102.16,	92.54,	-134.209
34,	-157.49,	90.68,	-104.984
35,	-142.02,	91.55,	-86.870];

JAMMER DATA SET case3

elseif(cno == 3)

%Jammer	Az (deg)	El (deg)	Power (dBW)
JA = [1,	-76.77,	92.65,	-95.774
2,	23.26,	94.46,	-134.784
3,	24.79,	95.14,	-119.621
4,	29.56,	94.74,	-121.159
5,	65.81,	93.48,	-139.728
6,	59.26,	93.68,	-134.207
7,	44.47,	94.12,	-133.237
8,	35.04,	94.26,	-134.430
9,	18.05,	94.18,	-89.827
10,	-2.45,	94.10,	-105.219
11,	49.79,	94.03,	-106.914
12,	40.04,	94.15,	-134.553
13,	23.41,	94.46,	-134.659
14,	-72.58,	93.10,	-124.408
15,	-27.10,	94.34,	-123.431
16,	42.63,	94.11,	-135.441
17,	49.82,	94.04,	-132.655
18,	-26.12,	94.52,	-122.364
19,	52.32,	93.87,	-134.385
20,	31.26,	95.02,	-119.738
21,	-25.06,	94.48,	-122.668
22,	24.05,	94.86,	-121.077
23,	-22.86,	94.13,	-123.494
24,	19.34,	94.45,	-86.865
25,	60.20,	93.63,	-135.178
26,	41.78,	94.37,	-105.597
27,	29.06,	95.21,	-119.121
28,	26.43,	94.93,	-120.423
29,	-9.30,	94.04,	-90.890
30,	-24.73,	94.51,	-122.550
31,	-23.15,	94.54,	-122.656
32,	31.61,	94.03,	-88.574
33,	3.78,	94.17,	-104.985];

REPORT DOCUMENTATION PAGE

Form Approved
OMB No. 0704-0188

Public reporting burden for this collection of information is estimated to average 1 hour per response, including the time for reviewing instructions, searching existing data sources, gathering and maintaining the data needed, and completing and reviewing the collection of information. Send comments regarding this burden estimate or any other aspect of this collection of information, including suggestions for reducing this burden, to Washington Headquarters Services, Directorate for Information Operations and Reports, 1215 Jefferson Davis Highway, Suite 1204, Arlington, VA 22202-4302, and to the Office of Management and Budget, Paperwork Reduction Project (0704-0188), Washington, DC 20503.

1. AGENCY USE ONLY (Leave blank)		2. REPORT DATE 14 May 2002		3. REPORT TYPE AND DATES COVERED Technical Report	
4. TITLE AND SUBTITLE Aperture Sampling Limitations of Linear and Circular Arrays for Direction Finding and Nulling				5. FUNDING NUMBERS C—F19628-00-C-0002	
6. AUTHOR(S) D.A. Shnidman					
7. PERFORMING ORGANIZATION NAME(S) AND ADDRESS(ES) Lincoln Laboratory, MIT 244 Wood Street Lexington, MA 02420-9108				8. PERFORMING ORGANIZATION REPORT NUMBER TR-1069	
9. SPONSORING/MONITORING AGENCY NAME(S) AND ADDRESS(ES) Department of Defense 9800 Savage Rd. Ft. George G. Meade, MD 20755-6000				10. SPONSORING/MONITORING AGENCY REPORT NUMBER ESC-TR-2001-063	
11. SUPPLEMENTARY NOTES None					
12a. DISTRIBUTION/AVAILABILITY STATEMENT Approved for public release; distribution is unlimited.				12b. DISTRIBUTION CODE	
13. ABSTRACT (Maximum 200 words) Antenna arrays are often used for direction finding and for suppressing spatially dependent interference. An upper limit to the number of useful elements in a specified aperture is shown to depend on element signal-to-noise ratio and processor precision. This report addresses relevant issues through eigenanalysis of a correlation matrix derived from a specific set of incoming wavefronts.					
14. SUBJECT TERMS				15. NUMBER OF PAGES 44	
				16. PRICE CODE	
17. SECURITY CLASSIFICATION OF REPORT Unclassified	18. SECURITY CLASSIFICATION OF THIS PAGE Unclassified	19. SECURITY CLASSIFICATION OF ABSTRACT Unclassified	20. LIMITATION OF ABSTRACT Same as Report		